Metastable supersolid in spin-orbit-coupled Bose-Einstein condensates

Wei-Lei Xia,[1,2,*] Lei Chen ,[1,3,*] Tian-Tian Li,[1,2] Yongping Zhang ,[4] and Qizhong Zhu [1,2,†]
[1]*Guangdong Provincial Key Laboratory of Quantum Engineering and Quantum Materials, School of Physics and Telecommunication Engineering, South China Normal University, Guangzhou 510006, China*
[2]*Guangdong-Hong Kong Joint Laboratory of Quantum Matter, Frontier Research Institute for Physics, South China Normal University, Guangzhou 510006, China*
[3]*School of Physics and Electronic Science, Zunyi Normal University, Zunyi 563006, China*
[4]*Department of Physics, Shanghai University, Shanghai 200444, China*

(Received 15 January 2023; accepted 24 April 2023; published 2 May 2023)

Supersolid is a special state of matter with both superfluid properties and spontaneous modulation of particle density. In this paper we focus on the supersolid stripe phase realized in a spin-orbit-coupled Bose-Einstein condensate and explore the properties of a class of metastable supersolids. In particular, we study a one-dimensional supersolid whose characteristic wave number k (magnitude of wave vector) deviates from k_m, i.e., the one in the ground state. In other words, the period of density modulation is shorter or longer than the one in the ground state. We find that this class of supersolids can still be stable if their wave numbers fall in the range $k_{c1} < k < k_{c2}$, with two thresholds k_{c1} and k_{c2}. Stripes with k outside this range suffer from dynamical instability with a complex Bogoliubov excitation spectrum at long wavelength. Experimentally, these stripes with k different from k_m are accessible by exciting the longitudinal spin dipole mode, resulting in temporal oscillation of the stripe period as well as k. Within the mean-field Gross-Pitaevskii theory, we numerically confirm that for a large enough amplitude of spin dipole oscillation, the stripe states become unstable through breaking periodicity, in qualitative agreement with the existence of thresholds of k for stable stripes. Our work extends the concept of supersolid and uncovers an unconventional class of metastable supersolids to explore.

DOI: 10.1103/PhysRevA.107.053302

I. INTRODUCTION

Supersolid is an exotic state of matter, which features both superfluid properties and spontaneous modulation of particle density. Supersolids are characterized by two types of gapless Goldstone modes, associated with spontaneous breaking of U(1) gauge symmetry and spatial translation symmetry, respectively. Previously, it had been long speculated that solid ^{4}He at low temperature could be a supersolid [1,2]; however, that idea was overturned by subsequent experiments [3,4]. In recent years, this concept has stimulated renewed interest among researchers due to significant progress made in the community of cold atomic gases. Until now, there have been three successful schemes to realize a supersolid, i.e., the stripe phase of a spin-orbit-coupled Bose-Einstein condensate (BEC) [5–11], a BEC coupled with modes of two optical cavities [12], and recently in dipolar gas with a roton excitation spectrum [13–19]. In addition, in spin-orbital angular-momentum-coupled quantum gases, there are also interesting supersolidlike stripe phases, i.e., the angular stripe phase [20–22].

A supersolid in its ground state and its low-energy excitations have been extensively studied, with particular attention paid to the existence of two types of gapless Goldstone modes [16,23–26]. These studies considered the collective excitations in the linear response regime, which reflects the properties of a supersolid close to the ground state. In fact, there are other classes of excited states of a supersolid. For example, in the plane-wave phase of a spin-orbit-coupled BEC, the wave vector does not necessarily coincide with the one in the ground state, but instead can take values different from the lowest-energy one. In particular, these states correspond to an excited state carrying mass current and under certain conditions they become a metastable superfluid [27–29]. Analogously, for the stripe phase, one can also vary the wave vector, or equivalently the period of the stripe, to realize a supersolid in the excited state [see Figs. 1(a) and 1(b)]. This scenario is also experimentally relevant as the supersolid prepared may not reach the ground state during the limited observation time. Will these supersolids be metastable? If not, what is the underlying instability mechanism? How can these metastable supersolids be experimentally accessed? These are the interesting questions we aim to answer in this paper.

To be specific, we focus on the supersolid realized in the stripe phase of a spin-orbit-coupled BEC and consider a supersolid whose wave number k (magnitude of wave vector) does not coincide with the one in the ground state, denoted by k_m, but instead a supersolid with general k. We find that nonlinear dispersion of the chemical potential with respect to k can exhibit a loop structure. For $k \neq k_m$, the supersolid is in the excited state and may not be stable. We study the stability of a general stripe state by calculating its Bogoliubov

*These authors contributed equally to this work.
†qzzhu@m.scnu.edu.cn

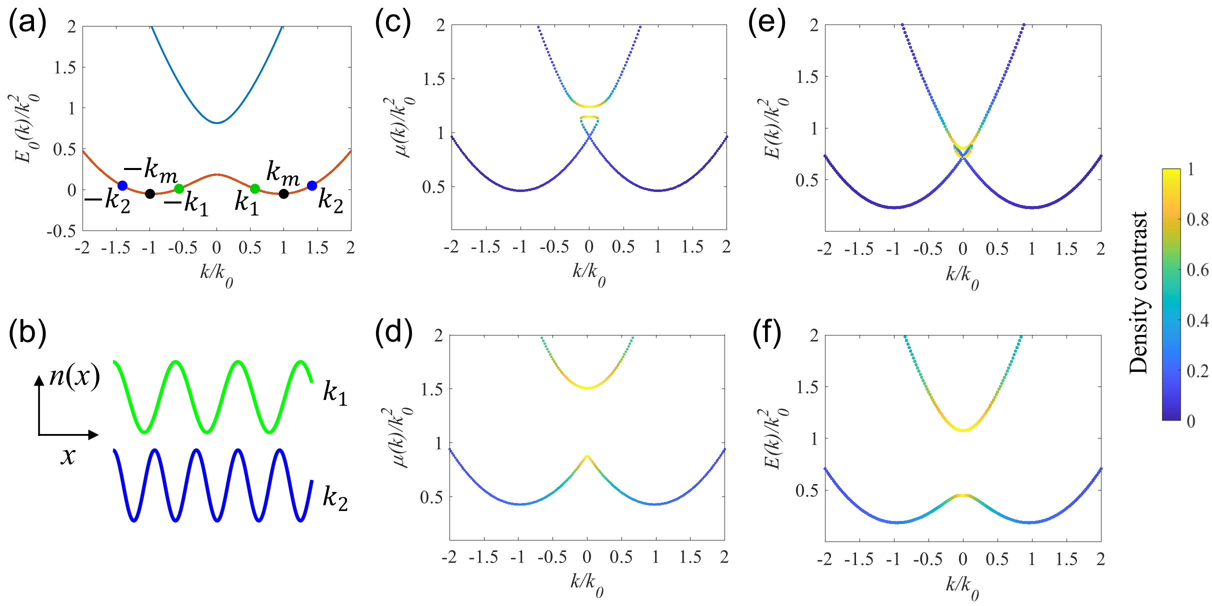

FIG. 1. (a) Noninteracting dispersion of spin-orbit-coupled BEC at small Ω. The black dots denote the momentum k_m of the plane wave in the ground state. The green (blue) dots denote the momentum of plane waves with momentum $k_1 < k_m$ ($k_2 > k_m$), whose interference results in a stripe with period longer (shorter) than the one in the ground state, as illustrated by their density modulations in (b). (c) and (d) Nonlinear dispersions of chemical potential $\mu(k)$ determined by Eq. (3). (e) and (f) Dispersions of energy $E(k)$ defined in Eq. (2) corresponding to (c) and (d), respectively. The line color in (c)–(f) denotes the density contrast $\mathcal{C}$, as shown by the color bar. The parameters are $\bar{n}g/k_0^2 = 0.484$, $\bar{n}g_{12}/k_0^2 = 0.44$, and (c) and (e) $\Omega/k_0^2 = 0.09$ and (a), (d), and (f) $\Omega/k_0^2 = 0.63$, with $\bar{n}$ the average condensate density.

excitation spectrum and find that stripe states with k within the range $k_{c1} < k < k_{c2}$ are metastable. When k falls outside this range, the supersolid suffers from dynamical instability. These stripes with $k \neq k_m$ can be accessed by exciting the longitudinal spin dipole mode of the stripe [30], and the thresholds of k are related to the upper limit of the oscillation amplitude of spin dipole mode.

The rest of this paper is organized as follows. In Sec. II we formulate the spin-orbit-coupled BEC within mean-field theory, numerically solve the wave function of the stripe state, and calculate the nonlinear dispersion $\mu(k)$ as a function of wave number k. In Sec. III we calculate the excitation spectrum of the stripe phase with Bogoliubov theory, from which we determine the stability condition of stripes and examine the instability mechanism. In Sec. IV we demonstrate that stripes with $k \neq k_m$ can be experimentally accessed by exciting the spin dipole mode, and the stability condition of the stripe obtained in Sec. III is related to the stability of the stripe in response to the spin dipole mode excitation within the framework of Gross-Pitaevskii theory. We summarize our results in Sec. V.

II. NONLINEAR DISPERSION

Spin-orbit-coupled BECs with equal Rashba and Dresselhaus types can be engineered by Raman coupling of two internal atomic states, as first experimentally realized by Lin *et al.* [31]. Assume that the Raman lasers introduce momentum transfer in the x direction and the trap frequencies in the y and z directions are high enough that the low-energy degree of freedom of this system can be described by the one-dimensional effective Hamiltonian with spin-orbit coupling

$$\hat{H}_0 = \frac{\hbar^2}{2m}(-i\partial_x - k_0\sigma_z)^2 + \frac{\Omega}{2}\sigma_x, \tag{1}$$

where k_0 is the strength of spin-orbit coupling, Ω is the Raman coupling strength, and Pauli matrices are defined in the pseudospin-$\frac{1}{2}$ Hilbert space. For simplicity, in the following calculations, we set $\hbar = m = 1$. Here k_0 and k_0^2 are chosen as the momentum and energy units, respectively. The dispersion of this Hamiltonian has two branches, as shown in Fig. 1(a).

Now consider that Bose-Einstein condensation occurs in this system and the two-component condensate can be described by the mean-field energy functional [32]

$$E(\Psi_\uparrow, \Psi_\downarrow) = \int dx (\Psi_\uparrow^*, \Psi_\downarrow^*)\hat{H}_0\begin{pmatrix}\Psi_\uparrow\\ \Psi_\downarrow\end{pmatrix} + g_{\uparrow\downarrow}|\Psi_\uparrow|^2|\Psi_\downarrow|^2 + \frac{g}{2}(|\Psi_\uparrow|^4 + |\Psi_\downarrow|^4). \tag{2}$$

Here $\Psi_\uparrow$ ($\Psi_\downarrow$) is the condensate wave function of the up (down) pseudospin and g (g_{12}) is the interaction strength between the same (different) spin species. The bare values of g and g_{12} are related to the s-wave scattering lengths between atoms of the same and different hyperfine states. For the ^{87}Rb atom, g and g_{12} are very close [31], making the density contrast of the stripe state very low [32]. However, their difference can be enhanced by various schemes, e.g., separating the two components in a bilayer configuration [33].

It is predicted that the ground state of this model has three phases, with the change of parameters such as Ω/k_0^2, g, and g_{12} [32]. For atomic density below a critical value, with the increase of Ω/k_0^2, the ground state changes from the stripe phase to the plane-wave phase and then to the zero-momentum phase. The stripe phase spontaneously breaks the translation symmetry of the Hamiltonian and develops periodic modulation of the atomic density, which is the focus of this paper.

Minimizing the energy functional with respect to the spinor wave function, one arrives at the stationary Gross-Pitaevskii (GP) equation

$$\mu\begin{pmatrix}\Psi_\uparrow\\ \Psi_\downarrow\end{pmatrix}=\begin{pmatrix}H_{\uparrow\uparrow} & \frac{\Omega}{2}\\ \frac{\Omega}{2} & H_{\downarrow\downarrow}\end{pmatrix}\begin{pmatrix}\Psi_\uparrow\\ \Psi_\downarrow\end{pmatrix}, \tag{3}$$

where $H_{\uparrow\uparrow}=(-i\partial_x-k_0)^2/2+g|\Psi_\uparrow|^2+g_{12}|\Psi_\downarrow|^2$ and $H_{\downarrow\downarrow}=(-i\partial_x+k_0)^2/2+g|\Psi_\downarrow|^2+g_{12}|\Psi_\uparrow|^2$. The wave function of a general stripe characterized by k has the form

$$\begin{pmatrix}\Psi_\uparrow\\ \Psi_\downarrow\end{pmatrix}=\sum_{n=-2L-1}^{2L+1}\begin{pmatrix}a_n\\ b_n\end{pmatrix}e^{inkx}, \tag{4}$$

where L is a positive integer and the spacing of integer n is 2. Note that for the stripe phase, apart from an overall phase factor, the coefficients satisfy the relation $b_n=a^*_{-n}$, i.e., they are symmetric under the simultaneous operation of space inversion and spin flip. Clearly, for the formation of periodic density modulation, a couple of plane waves are enough (e.g., only two plane waves with opposite momenta are used in the ansatz of Ref. [32]). Nevertheless, the eigenstates of the nonlinear equations should in general contain infinitely many plane waves because, e.g., starting from two plane waves with opposite momenta, the mean-field interaction term will become an effective periodic potential, which further induces coupling between more plane waves whose momenta differ by the reciprocal lattice vector ($2k$ here). So, in principle, the eigenstates should contain infinitely many plane waves similar to Bloch waves in periodic potentials, although in realistic calculations a finite cutoff L has to be taken. Plugging the above expansion into the stationary GP equation, one arrives at a set of nonlinear equations that the variables a_n, b_n, and μ satisfy. By solving the set of nonlinear equations, one can simultaneously obtain the nonlinear dispersion, i.e., μ as a function of k, and also the coefficients a_n and b_n of stripe wave function.

Figure 1 shows the nonlinear dispersion of both the chemical potential $\mu(k)$ and energy $E(k)$. It is clear that, at an optimal wave number k_m, the energy of the stripe state is the lowest. Here k_m is close to the one determined in the noninteracting model, i.e., $k_m=k_0\sqrt{1-\Omega^2/4k_0^4}$ [32]. In addition, k_m corresponds to an optimal period d_m of stripe density modulation, and since the minimum wave number of the stripe density is $2k_m$, one obtains the relation $d_m=\pi/k_m$. Away from k_m, the energy of the stripe state increases, and a loop or swallowtail structure appears in $\mu(k)$ near $k=0$ for small Ω, as shown in Fig. 1(c), similar to the plane-wave case [34]. The density contrast of the stripe state, defined as $\mathcal{C}\equiv(n_{\max}-n_{\min})/(n_{\max}+n_{\min})$, with $n_{\max}$ ($n_{\min}$) the local density maximum (minimum), at different k is also indicated by color. One can observe that stripes with small k or a long period have larger density contrast. Note that in this system, to experimentally confirm the existence of a supersolid, a direct measurement of the superfluid response is also required, e.g., using the method in Ref. [35], besides the detection of density modulation. We also find that the detailed structure of dispersion $\mu(k)$ depends on the cutoff L, but the lower branch of dispersion near k_m does not, which is the range of k we are interested in.

Previous studies only considered the stripe state with this optimal wave number k_m. Here we loosen this constraint and consider a general stripe with arbitrary k, corresponding to the ground state or excited states depending on whether $k=k_m$. For $k>k_m$, the stripe is effectively compressed with shorter period; otherwise, it is stretched. Since for $k\neq k_m$ these stripes are in the excited state, it is natural to ask whether or not these stripes are stable. In other words, does there exist a metastable supersolid? This is the issue we will address in the following section.

III. STABILITY OF SUPERSOLIDS

The stability of stripes in the excited state, or $k\neq k_m$, can be examined by studying their Bogoliubov excitation spectra. If the excitation spectrum at all excitation momenta is real and non-negative, these stripes are stable; otherwise, they suffer from Landau instability or dynamical instability [36].

We start from the time-dependent GP equation

$$i\frac{\partial}{\partial t}\begin{pmatrix}\Psi_\uparrow\\ \Psi_\downarrow\end{pmatrix}=\begin{pmatrix}H_{\uparrow\uparrow} & \frac{\Omega}{2}\\ \frac{\Omega}{2} & H_{\downarrow\downarrow}\end{pmatrix}\begin{pmatrix}\Psi_\uparrow\\ \Psi_\downarrow\end{pmatrix} \tag{5}$$

and study the stability of these stripe states with respect to weak perturbations. Due to periodic modulation of the density, the eigenmodes of perturbation take the form of Bloch waves

$$\begin{pmatrix}\delta\Psi_\uparrow\\ \delta\Psi_\downarrow\end{pmatrix}=e^{-i\mu(k)t}\sum_{n=-2L-1}^{2L+1}\begin{pmatrix}u_n^\uparrow\\ u_n^\downarrow\end{pmatrix}e^{i(nk+q)x}e^{-i\varepsilon(q)t}+e^{-i\mu(k)t}\sum_{n=-2L-1}^{2L+1}\begin{pmatrix}v_n^{\uparrow *}\\ v_n^{\downarrow *}\end{pmatrix}e^{i(nk-q)x}e^{i\varepsilon(q)t}, \tag{6}$$

where $u_n^{\uparrow\,(\downarrow)}$ and $v_n^{\uparrow\,(\downarrow)}$ are perturbation amplitudes for the spin-up (-down) component and q is the excitation momentum. Writing $\Psi'_\sigma=\Psi_\sigma+\delta\Psi_\sigma$, plugging Ψ'_σ into the time-dependent GP equation, and only retaining the linear term of perturbation, one arrives at the Bogoliubov equation that $u_n^{\uparrow\,(\downarrow)}$ and $v_n^{\uparrow\,(\downarrow)}$ satisfy and obtains the excitation spectrum $\varepsilon(q)$ as well.

The excitation spectra of stripes at different k are depicted in Fig. 2. Due to periodic density modulation, the excitation spectrum $\varepsilon(q)$ has a feature similar to the Bloch band of periodic potentials. For a stripe in the ground state, i.e., $k=k_m$, the excitation spectrum features two branches of real and non-negative gapless excitations [see Fig. 2(d)], corresponding to two Goldstone modes associated with spontaneous breaking of U(1) gauge symmetry and translation symmetry [23]. With the deviation of k from k_m, the lower branch of the excitation spectrum becomes softer [Figs. 2(c) and 2(e)]. For $k_{c1}<k<k_{c2}$, with k_{c1} and k_{c2} the lower and upper threshold, respectively, the feature of real and non-negative excitations remains, which defines a metastable supersolid. When $k<k_{c1}$ or $k>k_{c2}$, the excitation spectrum becomes complex at small q, signaling the dynamical instability of those stripes

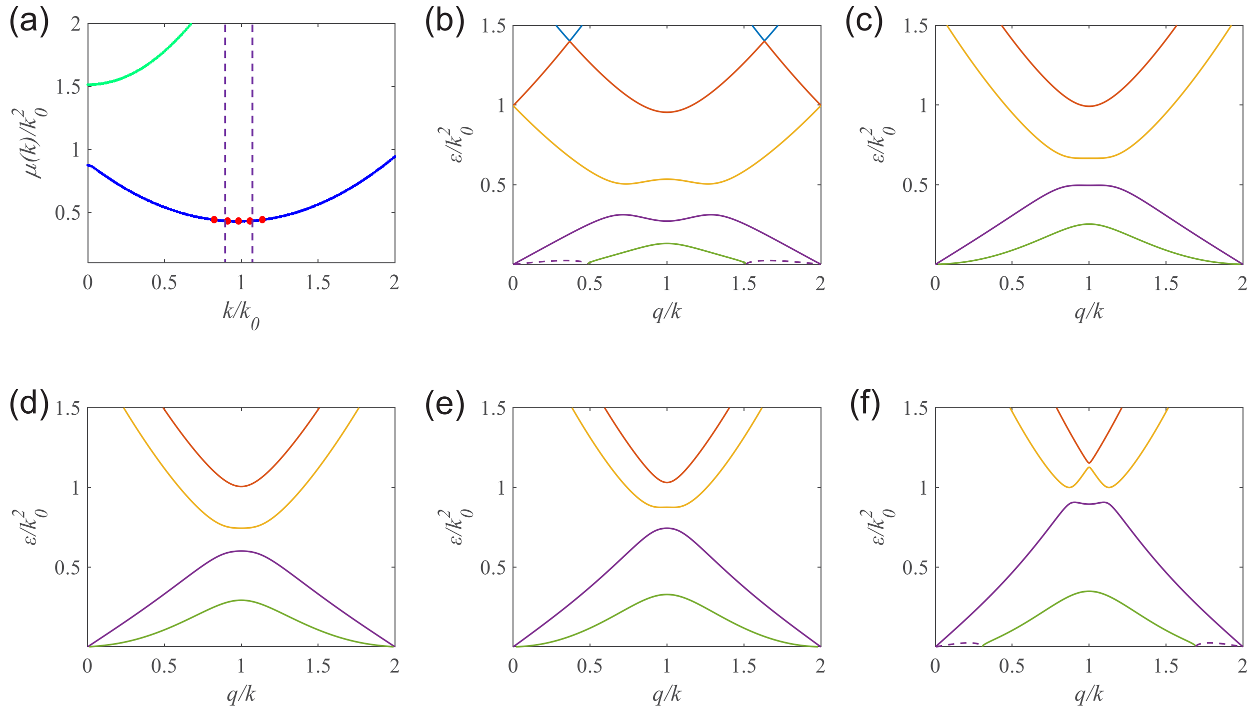

FIG. 2. (a) Dispersion $\mu(k)$ with five characteristic momenta k, denoted by red dots. From left to right, they correspond to k in (b)–(f). The dashed lines indicate the lower and upper thresholds of k of stable stripes. (b)–(f) Bogoliubov excitation spectra for stripes with $k/k_0 = 0.76, 0.9, 0.96, 1.04, 1.16$ [denoted by red dots in (a)], corresponding to $k < k_{c1}$, $k_{c1} < k < k_m$, $k = k_m$, $k_m < k < k_{c2}$, and $k > k_{c2}$, respectively. Excitation spectra in (c)–(e) are all real and non-negative. Dashed lines in (b) and (f) denote the imaginary parts of complex excitation spectra. The other parameters are $\bar{n}g/k_0^2 = 0.484$, $\bar{n}g_{12}/k_0^2 = 0.44$, and $\Omega/k_0^2 = 0.59$.

[Figs. 2(b) and 2(f)]. We find that the excitation spectrum always turns complex starting from $q \to 0$, indicating that instability first appears in the long-wavelength excitation. Note here that we do not find Landau instability or energetic instability, i.e., real and negative excitations, and this seems a common feature in various superfluids with counterflow characteristic [37–39]. In addition, in practical calculations, we have set $L = 2$ (six momenta in the summation) in the solution of both the stripe wave function and excitation spectrum and have checked that a larger L only introduces a negligible difference.

Both k_{c1} and k_{c2} depend on the Raman coupling strength and the interaction strengths g and g_{12}. Figure 3 shows the change of two thresholds k_{c1} and k_{c2} as functions of Ω/k_0^2 for two sets of interaction strengths. One can find that, in both Figs. 3(a) and 3(b), k_{c1} and k_{c2} are getting closer to each other with the increase of Ω/k_0^2, when approaching the stripe and plane-wave phase boundary [32]. In addition, k_{c1} and k_{c2} almost lie symmetrically on opposite sides of k_m. The range of stable k becomes narrower, consistent with the expectation that the stripe states are more susceptible to dynamical instability when approaching the phase boundary. A comparison between Figs. 3(a) and 3(b) also shows that the larger ratio g/g_{12} leads to a wider range of k of stable stripes.

IV. EXPERIMENTAL OBSERVATION

A stripe with k different from k_m can be accessed by exciting the spin dipole mode of spin-orbit-coupled BEC, which is associated with the temporal change of stripe period [30]. Analogously, to examine the stability of the plane-wave phase in a spin-orbit-coupled BEC, it was previously proposed to excite the dipole oscillation of the condensate, whose center-of-mass momentum sweeps over a finite range around the minimum of dispersion [29,40].

Here the spin dipole mode can be excited by first preparing the stripe in the ground state with the perturbation $-\omega^2 x_0 x \sigma_z$ added to the Hamiltonian and then suddenly releasing the perturbation and observing the temporal evolution of the stripe wave function as well as oscillation of the density modulation

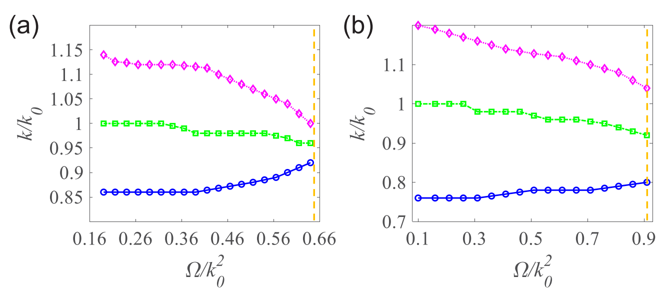

FIG. 3. Change of upper and lower thresholds k_{c1} and k_{c2} with respect to Ω denoted by lines with pink diamonds and blue circles, respectively. The change of k_m is shown by the green line with squares for comparison. Vertical orange dashed lines indicate the critical value of Ω, beyond which the stripe phase is not the ground state. The critical Ω is (a) 0.6473 and (b) 0.9123. The other parameters are (a) $\bar{n}g/k_0^2 = 0.484$ and $\bar{n}g_{12}/k_0^2 = 0.44$ and (b) $\bar{n}g/k_0^2 = 0.57$ and $\bar{n}g_{12}/k_0^2 = 0.456$.

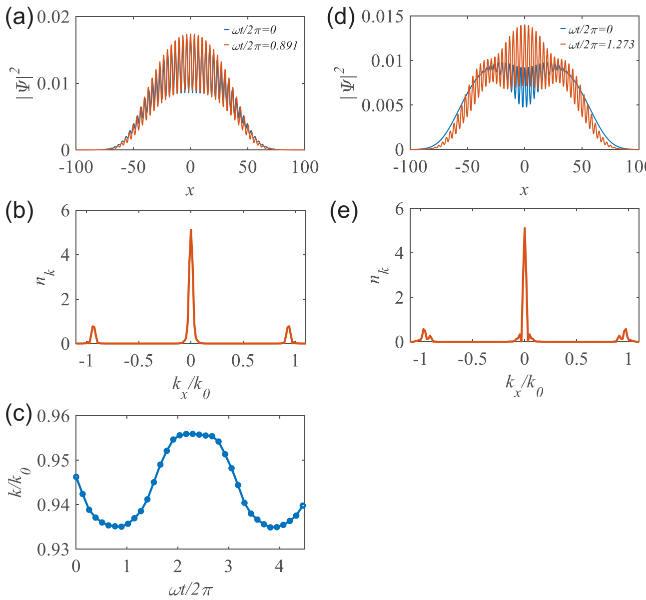

FIG. 4. (a) Overall density at two moments specified in the legend, for a small initial displacement $x_0 = 2.5$. The stripe has a well-defined period and k in this case, with (b) momentum distribution at $\omega t/2\pi = 0.891$. (c) Temporal oscillation of k. (d) Overall density for a large initial $x_0 = 25$, with (e) its momentum distribution at $\omega t/2\pi = 1.273$. The period and k of the stripe are not well defined in this case. The momentum distribution is obtained by a Fourier transform of the density, with momentum divided by 2 for comparison with k defined in this work. The trap frequency is $\omega/k_0^2 = 0.002$. The other parameters are $\bar{n}g/k_0^2 = 0.484$, $\bar{n}g_{12}/k_0^2 = 0.44$, and $\Omega/k_0^2 = 0.647$, the same as in Fig. 3(a).

period or k [30]. Numerically, we first find the ground state of the system with the perturbation $-\omega^2 x_0 x\sigma_z$ and a harmonic trap $V(x) = \omega^2 x^2/2$ by evolving the GP equation in imaginary time. In this way, the spin-up or -down component of the stripe is shifted in opposite directions in the ground state. Subsequently, at time $t = 0$, the perturbation is released and the real time evolution of stripe is obtained with the time-dependent GP equation

$$i\frac{\partial}{\partial t}\begin{pmatrix}\Psi_\uparrow \\ \Psi_\downarrow\end{pmatrix} = \begin{pmatrix}H_{\uparrow\uparrow} & \frac{\Omega}{2} \\ \frac{\Omega}{2} & H_{\downarrow\downarrow}\end{pmatrix}\begin{pmatrix}\Psi_\uparrow \\ \Psi_\downarrow\end{pmatrix}, \tag{7}$$

where $H_{\uparrow\uparrow} = (-i\partial_x - k_0)^2/2 + g|\Psi_\uparrow|^2 + g_{12}|\Psi_\downarrow|^2 + V(x)$ and $H_{\downarrow\downarrow} = (-i\partial_x + k_0)^2/2 + g|\Psi_\downarrow|^2 + g_{12}|\Psi_\uparrow|^2 + V(x)$.

Figures 4(a) and 4(d) depict the overall density distribution $|\Psi|^2$ of the stripe at two different moments for two different initial displacements x_0. Also shown are the momentum distribution obtained by a Fourier transform of the overall density [Figs. 4(b) and 4(e)] and the oscillation of k with time [Fig. 4(c)]. We find that, for a small initial displacement x_0, the overall profile of the density remains similar and the momentum distribution always features a peak centered at $k_x = 0$ and a pair of peaks centered at $k_x = \pm k$ associated with stripe period, as shown in Figs. 4(a) and 4(b). In this case, the stripe has well-defined periodicity and the oscillation amplitude of k around k_m is small, lying within the stable regime in Fig. 3(a) (see the orange dashed line within the stable range). The oscillation behavior of k is consistent with recent studies [30]. On the other hand, for large initial x_0, the momentum distribution develops multiple peaks centered at nonzero momentum, which means the crucial feature of the stripe is destroyed with no definite period, as shown in Figs. 4(d) and 4(e). This behavior qualitatively confirms our expectation that, when the oscillation magnitude of k is large for large initial x_0, the stripe can suffer from dynamical instability, with a significant change in the feature of the density distribution. So the stability region of k effectively corresponds to a limit on the amplitude of the spin dipole oscillation. Note also that the agreement here is qualitative, as there is a harmonic trap included in the time evolution of the GP equation but not present in the calculation of the Bogoliubov excitation spectrum. The agreement should be better for a weaker trap with harmonic-oscillator length a_x much larger than the stripe period.

V. CONCLUSION

In summary, we have studied the properties of a class of metastable supersolid stripes in spin-orbit-coupled BECs. We found that for a stripe with a general wave number k, the nonlinear dispersion $\mu(k)$ can exhibit a loop structure. In addition, when the wave number k of stripes deviates from the one in the ground state, supersolids can still be stable with respect to low-energy excitations. There exist two thresholds k_{c1} and k_{c2}, and for stripes with $k_{c1} < k < k_{c2}$, their Bogoliubov excitation spectra are always real and non-negative. For stripes with k outside this regime, the excitation spectrum at long wavelength becomes complex, signaling the dynamical instability of those stripes. We also point out that the thresholds of k for stable stripes are related to the stability criteria of stripes in response to spin dipole oscillation, which is accompanied by temporal oscillation of k. For spin dipole oscillation of large amplitude, the dramatic change in the feature of stripe wave functions can be qualitatively explained by the instability mechanism we propose here. With the recent experimental progress on compressional oscillations in dipolar supersolids [17], it will be interesting to explore similar stability properties there.

ACKNOWLEDGMENTS

W.-L.X., T.-T.L., and Q.Z. were supported by the National Key Research and Development Program of China (Grant No. 2022YFA1405304), the National Natural Science Foundation of China (Grant No. 12004118), and the Guangdong Basic and Applied Basic Research Foundation (Grants No. 2020A1515110228 and No. 2021A1515010212). L.C. was supported by the National Natural Science Foundation of China (Grant No. 12264061) and the Science Foundation of Guizhou Science and Technology Department (Grant No. QKHJZ[2021]033). Y.Z. was supported by the National Natural Science Foundation of China through Grants No. 11974235 and No. 11774219.

[1] E. Kim and M. H. W. Chan, Nature (London) **427**, 225 (2004).
[2] E. Kim and M. H. W. Chan, Science **305**, 1941 (2004).
[3] J. Day and J. Beamish, Nature (London) **450**, 853 (2007).
[4] D. Y. Kim and M. H. W. Chan, Phys. Rev. Lett. **109**, 155301 (2012).
[5] C. Wang, C. Gao, C.-M. Jian, and H. Zhai, Phys. Rev. Lett. **105**, 160403 (2010).
[6] T.-L. Ho and S. Zhang, Phys. Rev. Lett. **107**, 150403 (2011).
[7] J.-R. Li, J. Lee, W. Huang, S. Burchesky, B. Shteynas, F. Ç. Top, A. O. Jamison, and W. Ketterle, Nature (London) **543**, 91 (2017).
[8] X.-L. Chen, J. Wang, Y. Li, X.-J. Liu, and H. Hu, Phys. Rev. A **98**, 013614 (2018).
[9] T. M. Bersano, J. Hou, S. Mossman, V. Gokhroo, X.-W. Luo, K. Sun, C. Zhang, and P. Engels, Phys. Rev. A **99**, 051602(R) (2019).
[10] A. Putra, F. Salces-Cárcoba, Y. Yue, S. Sugawa, and I. B. Spielman, Phys. Rev. Lett. **124**, 053605 (2020).
[11] J. Sánchez-Baena, J. Boronat, and F. Mazzanti, Phys. Rev. A **101**, 043602 (2020).
[12] J. Léonard, A. Morales, P. Zupancic, T. Esslinger, and T. Donner, Nature (London) **543**, 87 (2017).
[13] L. Tanzi, E. Lucioni, F. Famà, J. Catani, A. Fioretti, C. Gabbanini, R. N. Bisset, L. Santos, and G. Modugno, Phys. Rev. Lett. **122**, 130405 (2019).
[14] F. Böttcher, J.-N. Schmidt, M. Wenzel, J. Hertkorn, M. Guo, T. Langen, and T. Pfau, Phys. Rev. X **9**, 011051 (2019).
[15] L. Chomaz, D. Petter, P. Ilzhöfer, G. Natale, A. Trautmann, C. Politi, G. Durastante, R. M. W. van Bijnen, A. Patscheider, M. Sohmen, M. J. Mark, and F. Ferlaino, Phys. Rev. X **9**, 021012 (2019).
[16] M. Guo, F. Böttcher, J. Hertkorn, J.-N. Schmidt, M. Wenzel, H. P. Büchler, T. Langen, and T. Pfau, Nature (London) **574**, 386 (2019).
[17] L. Tanzi, S. M. Roccuzzo, E. Lucioni, F. Famà, A. Fioretti, C. Gabbanini, G. Modugno, A. Recati, and S. Stringari, Nature (London) **574**, 382 (2019).
[18] M. A. Norcia, C. Politi, L. Klaus, E. Poli, M. Sohmen, M. J. Mark, R. N. Bisset, L. Santos, and F. Ferlaino, Nature (London) **596**, 357 (2021).
[19] D. Petter, A. Patscheider, G. Natale, M. J. Mark, M. A. Baranov, R. van Bijnen, S. M. Roccuzzo, A. Recati, B. Blakie, D. Baillie, L. Chomaz, and F. Ferlaino, Phys. Rev. A **104**, L011302 (2021).
[20] X.-L. Chen, S.-G. Peng, P. Zou, X.-J. Liu, and H. Hu, Phys. Rev. Res. **2**, 033152 (2020).
[21] K.-J. Chen, F. Wu, J. Hu, and L. He, Phys. Rev. A **102**, 013316 (2020).
[22] S.-G. Peng, K. Jiang, X.-L. Chen, K.-J. Chen, P. Zou, and L. He, AAPPS Bull. **32**, 36 (2022).
[23] Y. Li, G. I. Martone, L. P. Pitaevskii, and S. Stringari, Phys. Rev. Lett. **110**, 235302 (2013).
[24] G. Natale, R. M. W. van Bijnen, A. Patscheider, D. Petter, M. J. Mark, L. Chomaz, and F. Ferlaino, Phys. Rev. Lett. **123**, 050402 (2019).
[25] G.-Q. Li, X.-W. Luo, J. Hou, and C. Zhang, Phys. Rev. A **104**, 023311 (2021).
[26] K. T. Geier, G. I. Martone, P. Hauke, and S. Stringari, Phys. Rev. Lett. **127**, 115301 (2021).
[27] Q. Zhu, C. Zhang, and B. Wu, Europhys. Lett. **100**, 50003 (2012).
[28] W. Zheng, Z.-Q. Yu, X. Cui, and H. Zhai, J. Phys. B **46**, 134007 (2013).
[29] T. Ozawa, L. P. Pitaevskii, and S. Stringari, Phys. Rev. A **87**, 063610 (2013).
[30] K. T. Geier, G. I. Martone, P. Hauke, W. Ketterle, and S. Stringari, Phys. Rev. Lett. **130**, 156001 (2023).
[31] Y.-J. Lin, K. Jiménez-García, and I. B. Spielman, Nature (London) **471**, 83 (2011).
[32] Y. Li, L. P. Pitaevskii, and S. Stringari, Phys. Rev. Lett. **108**, 225301 (2012).
[33] G. I. Martone, Y. Li, and S. Stringari, Phys. Rev. A **90**, 041604(R) (2014).
[34] Y. Zhang, Z. Gui, and Y. Chen, Phys. Rev. A **99**, 023616 (2019).
[35] R. Onofrio, C. Raman, J. M. Vogels, J. R. Abo-Shaeer, A. P. Chikkatur, and W. Ketterle, Phys. Rev. Lett. **85**, 2228 (2000).
[36] B. Wu and Q. Niu, New J. Phys. **5**, 104 (2003).
[37] C. K. Law, C. M. Chan, P. T. Leung, and M.-C. Chu, Phys. Rev. A **63**, 063612 (2001).
[38] S. Ishino, M. Tsubota, and H. Takeuchi, Phys. Rev. A **83**, 063602 (2011).
[39] Q. Zhu, Q.-f. Sun, and B. Wu, Phys. Rev. A **91**, 023633 (2015).
[40] J.-Y. Zhang, S.-C. Ji, Z. Chen, L. Zhang, Z.-D. Du, B. Yan, G.-S. Pan, B. Zhao, Y.-J. Deng, H. Zhai, S. Chen, and J.-W. Pan, Phys. Rev. Lett. **109**, 115301 (2012).